Preprint
UCRL-JC-138807

Progress with the Lick Adaptive Optics System

D.T. Gavel, S.S. Olivier, B. Bauman, C.E. Max, B. Macintosh

This article was submitted to SPIE International Symposium on Astronomical Telescopes and Instrumentation 2000, Munich, Germany, March 27-31, 2000

March 1, 2000

U.S. Department of Energy

Lawrence
Livermore
National
Laboratory

This work was performed under the auspices of the United States Department of Energy by the University of California, Lawrence Livermore National Laboratory under contract No. W-7405-Eng-48.

Progress with the Lick Adaptive Optics system

Donald T. Gavel, Scot S. Olivier, Brian Bauman, Claire E. Max, Bruce Macintosh

Lawrence Livermore National Laboratory, Livermore, CA

ABSTRACT

Progress and results of observations with the Lick Observatory Laser Guide Star Adaptive Optics System are presented. This system is optimized for diffraction-limited imaging in the near infrared, 1-2 micron wavelength bands. We describe our development efforts in a number of component areas including, a redesign of the optical bench layout, the commissioning of a new infrared science camera, and improvements to the software and user interface. There is also an ongoing effort to characterize the system performance with both natural and laser guide stars and to fold this data into a refined system model. Such a model can be used to help plan future observations, for example, predicting the point-spread function as a function of seeing and guide star magnitude.

1. INTRODUCTION

An important goal of the adaptive optics project at Lick Observatory is to make the AO system a robust facility instrument useful for routine astronomical observations. To this end, the system has undergone extensive redevelopment and testing during the previous year. The optical layout was modified to improve stability and allow a larger field of view[1]. Also, much of the user interface and motor control software was rewritten to make observing more automated and efficient. Coupled with these changes, a new infrared science camera was commissioned. The new camera, called IRCAL (InfraRed CAmera at Lick) was developed under the leadership of Professor James Graham of U.C. Berkeley[2]. It has a pixel scale and cold pupil stop optimized for the Lick AO system's f/28.6 output beam.

The AO system, with IRCAL, was used extensively by astronomers in science observing programs in 1999. Targets ranged from planets in our solar system to galaxies. The AO system provides corrected images at the diffraction-limit of the 3 meter Shane Telescope in the near infrared bands, 1.0 to 2.2 microns. This is an order of magnitude better than uncorrected seeing at Lick.

Ongoing engineering work at Lick includes characterizing the closed loop AO system performance under a variety of seeing conditions with the goal being to develop a set of measurement-based observation planning tools[3]. This work demands that we gain a reasonably complete understanding of the system's point spread function formation process both in the spatial and temporal domain. Sections 4 and 5 shows results of Strehl performance modeling and measurements of the point-spread function.

The laser guide star has demonstrated its utility as a beacon for the higher order AO loop. We have attained closed loop Strehls as high as 0.49[4]. Over the past two years, there has been a significant effort to tune the laser system for better beam quality and to refine the diagnostics for measuring the beam properties. On-sky testing and analysis have provided insight into the beacon's apparent size and the impact on system performance[5,6]. A review of these results is given in section 6. Further engineering work on the laser and beam launch system will continue this year with the goal of making the laser guide star routinely useful for science observations.

2. SYSTEM UPGRADES

2.1 Optical Bench Layout

The optical layout in the original Lick prototype system split the guide star and science beams in collimated space, sending the science light to an f/29 focusing parabola for the science camera and the beacon light to an f/6 focusing parabola for the wavefront sensor. This arrangement introduced difficulties in calibration since the two parabolas were in non-common beam paths; any slight misalignment would introduce wavefront errors that cannot be sensed and corrected by the AO system. Secondly, the f/6 beam for the wavefront sensor (originally chosen fast in order to save space on the table) put untenable

mechanical tolerance and size requirements on components in the wavefront sensor, making it difficult to keep the sensor stably aligned.

The new layout splits the light in the f/29 converging beam (Figure 1). With this arrangement, the f/6 beam and non-common path parabolas are eliminated. The wavefront sensor's collimating and relay optics were redesigned and mounted with large, good quality stages. With the slower guide star beam there is a factor of five decrease in the tolerance required for positioning an iris at the guide star focus (this iris blocks the laser Rayleigh scatter, or a troublesome binary companion to a natural guide star). Added room at the focus also allowed us to put in a more stable iris stage and fit it with motors for x-y positioning and closure.

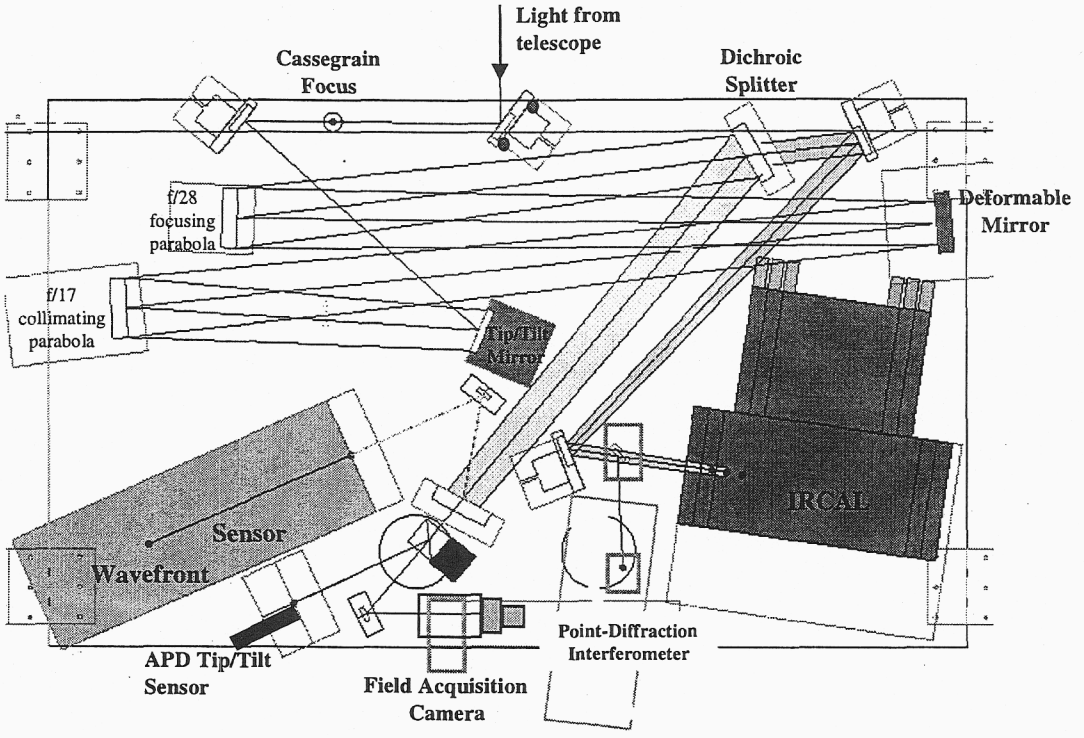

Figure 1 Optical layout of the Lick Adaptive Optics system

2.2 Field Steering

A particularly important improvement to the layout was the introduction of motorized field-steering mirrors in the guide star path. These allow the wavefront sensor to be "positioned" to an off-axis point in the field where a natural guide star might be located, while the science camera remains boresited to the telescope. Typical IR observation involves nodding the telescope so that the science image can be placed in different locations on the IR sensor array. The positioning of the field-steering mirrors drives the nod in the following manner. In closed-loop, long-term average tip/tilt mirror drive is offloaded to the telescope guider to keep the tip/tilt mirror from exceeding its actuation range. When the field-steering mirrors are adjusted, such a signal appears on the tip/tilt mirror and the telescope is driven to compensate, i.e. it nods. The field-steering control system is calibrated so that predictable nodding can be performed.

The optical path up to the field-steering mirrors has been designed to have a 2 arcminute diameter unvignetted field of view, so that guide stars can be chosen up to 1 arcminute off axis. The first field steering "mirror" can be a dichroic or 90/10 splitter, so that the entire field is sent on to a field acquisition camera. This camera is a Photometrics CCD with a wide field lens that allows coverage of the entire field at 0.28 arcsecond/pixel. The wide field lens can be positioned out of the way so that the camera doubles as a point-spread analysis and calibration sensor at 0.016 arcseconds/pixel. The camera sits on a focus stage, which allows it to take in and out of focus exposures of the point source simulator. This data is used for internal wavefront calibration and initial flattening of the deformable mirror via the Gerchberg-Saxton phase diversity procedure[7].

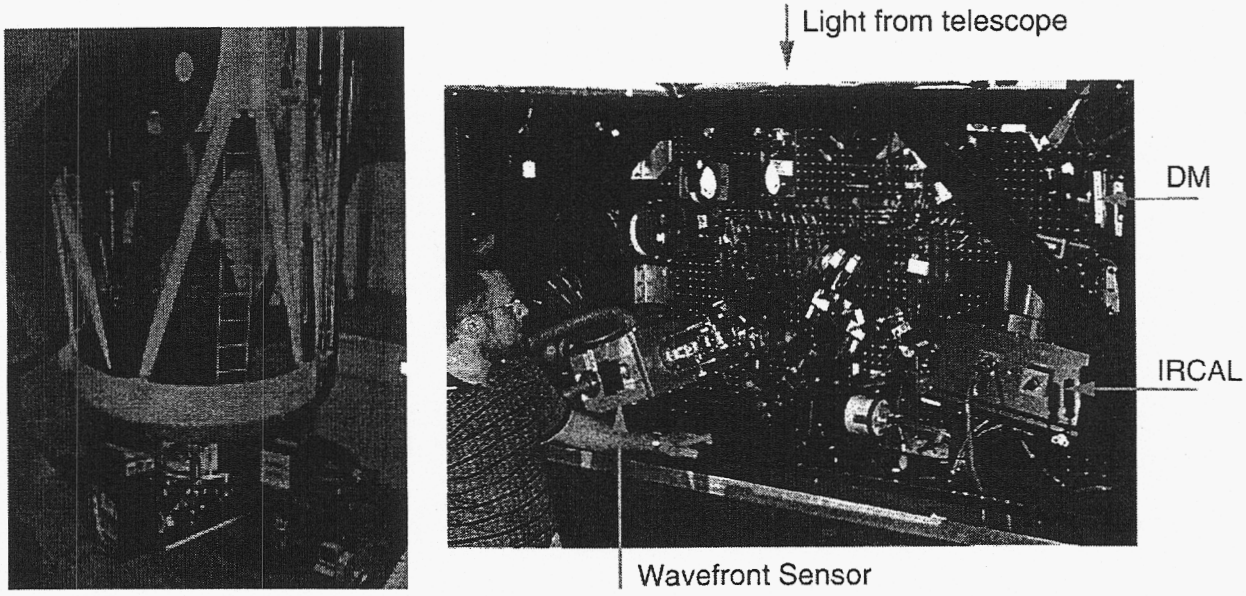

Figure 2. Left: the AO optical bench is shown mounted at the Cassegrain focus of the Shane 3 meter telescope. Right: a close-up of the optical bench shows the wavefront sensor camera, IRCAL science camera, and field acquisition camera. The deformable mirror is difficult to see, but is located in the upper right, above IRCAL.

2.3 Software

The software and user interface was completely redesigned to streamline AO system setup/calibration and observing. The AO system can now be operated remotely from one Unix/X-Windows console using a set of Tcl/Tk graphical user interfaces (GUIs). This system controls all the motors both individually or in combination for automated observing sequences, the most notable of which is nodding, and provides an interface to the real-time controller for setting controller parameters and opening and closing the AO loops. The software also accepts commands via socket communications with the science instrument. For example, IRCAL can coordinate its exposures with the AO system by sending nod and open/close loop commands through the Lick instrument communication protocol, TRAFFIC. The AO software communicates with the telescope control system, TELCO, to gather and display RA and DEC information. The software provides an automated log and generates FITS card information for the science image files.

3. NEW INFRARED SCIENCE IMAGING CAMERA: IRCAL

IRCAL (InfraRed CAmera for Lick) saw its first light on the AO system in November 1998. During engineering nights in June and July 1999, we continued to characterize the camera for sensitivity and noise performance. Figure 3 shows preliminary sensitivity curves.

IRCAL uses a 256x256 Rockwell PICNIC array (similar to a NICMOS-3 detector) which is sensitive from 0.9 - 2.5 microns. The pixel scale is 0.076 arcseconds/pixel, Nyquist sampled at 2.2 microns, providing a 19.4 arcsecond square field of view. IRCAL is equipped with a standard suite of near-IR photometric filters. Work is in progress to equip IRCAL with a coronagraph and grisms. We anticipate that a simple coronagraph will be available in the summer of 2000. An R=500 long-slit grism exists. In addition a cross-dispersed R ~ 4000 mode covering the entire K-window will be available within the coming year.

Additional details about IRCAL's design and testing can be found in the companion paper[2].

During engineering tests in August 1999, we analyzed the point spread function of IRCAL / closed loop AO, both on an internal calibration source and on a point-source star. These results are discussed in section 5 below.

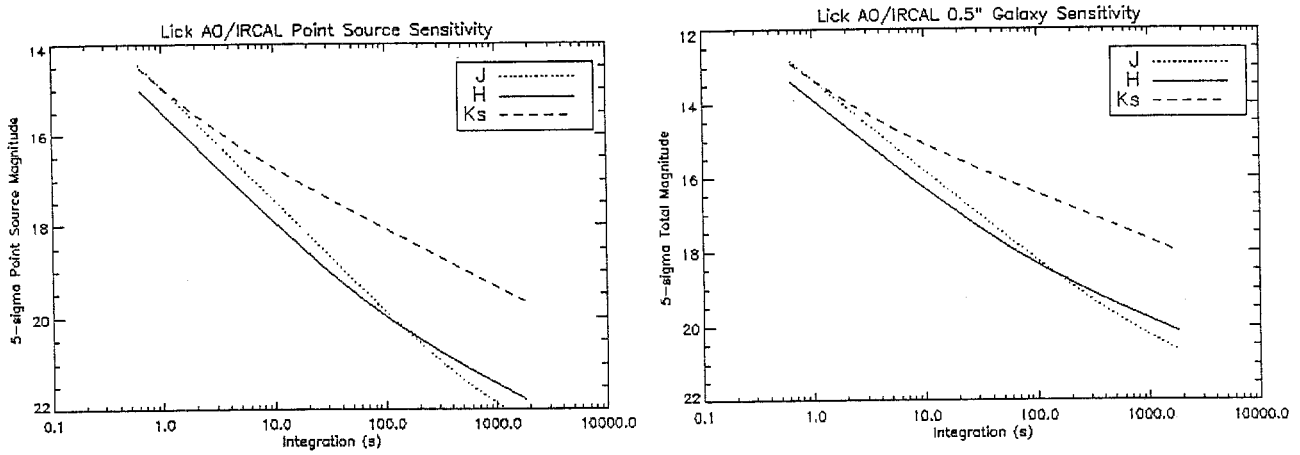

Figure 3. Sensitivity curves for IRCAL. Left: point source sensitivity shown as exposure time needed to reach signal-to-noise of 5. Sky background is higher in K_S band, whereas in J, the signal is lower since the AO system has lower Strehl at shorter wavelengths. Right: sensitivity curves for an extended source, such as a galaxy.

4. CLOSED LOOP AO PERFORMANCE I: STREHL

We use the approximation for closed loop Strehl ratio

$$S = e^{-\sigma_\phi^2} \tag{1}$$

where the wavefront phase variance is a sum of contributing terms:

$$\sigma_\phi^2 = \sigma_{DM}^2 + \sigma_{servo}^2 + \sigma_{meas}^2 + \sigma_{aniso}^2 + \sigma_{cal}^2 \tag{2}$$

Table 1 shows a typical error budget for the AO system with both natural and laser guide stars. The error budget model was developed based on data gathered during the 1998 and 1999 observing campaigns and has been shown to reliably predict the Strehl given the seeing. The error budget model was used to generate the Strehl prediction curves shown in Figure 4, which are useful for planning natural guide star observations. In 2000, we plan to collect a larger dataset of open and closed loop images along with system telemetry data in order to characterize the telescope's seeing conditions statistically and to correlate AO system performance to the seeing conditions.

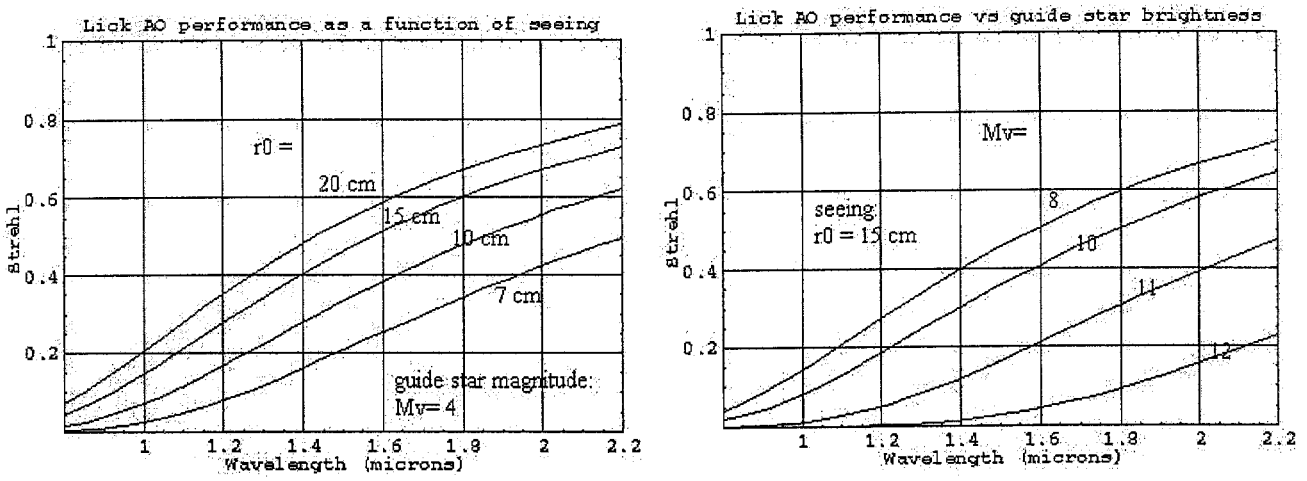

Figure 4. Strehl prediction curves for natural guide stars

Table 1. AO error budgets for typical conditions at Lick

Term	Formula	Determining factors	On-axis natural guide star	Laser guide star
DM	$\mu(d/r_0)^{5/3}$	Seeing, r_0 Actuator spacing, d Mirror response function, μ	r_0=12 cm d=44 cm μ=0.26 σ_{DM} = 148 nm	148 nm
Servo	$\kappa(f_g/f_c)^{5/3}$	Greenwood frequency f_g, Control bandwidth, f_c	f_g=50 Hz f_c=20 Hz $\kappa(D/r_0)$=0.24 σ_{servo}=89 nm	fg=50 Hz fc=10 Hz σ_{servo}=166 nm
Measurement	$\left(\chi\eta F\cdot\frac{1}{SNR}\right)^2$	Signal-to-noise, *SNR* Spot size, *F* Reconstructor noise propagator, η Closed-loop transfer function, χ	m_V=9 (SNR=7) *F*=0.5" (eq. 3) χ=0.4 η=0.6 σ_{meas}=87 nm	P_{laser}=18 W (SNR=13) *F*=1.9" (eq. 3) σ_{meas}=170 nm
Anisoplanatism	$(\theta/\theta_0)^{5/3}$ $(D/d_0)^{5/3}$	Off-axis distance, θ Anisoplanatic patch, θ_0 (NGS) Focal anisoplanatic size, d_0 (LGS)	(on-axis)	d_0=5 m D=3 m σ_{FA}=56 nm
Calibration		DM flattening	σ_{cal}=100 nm	σ_{cal}=100 nm
Total			σ_ϕ=215 nm S(λ=2μ) = 0.63	σ_ϕ=301 nm S(λ=2μ) = 0.41

5. CLOSED LOOP AO PERFORMANCE II: PSF

5.1 Internal calibration

We have made substantial efforts to improve system internal calibration. Internal wavefront error is a significant component of the closed-loop error and there is still room for improvement. Internal wavefront is dominated by the non-flatness of the deformable mirror. We currently use two alternative methods to measure the wavefront, phase diversity[7] and interferometry[8,9], then send correction offsets to the deformable mirror actuators so as to null the phase error. This has been shown to successfully reduce internal wavefront errors to about 100 nm rms. Figure 5 shows an internal PSF comparing it to the theoretical perfect PSF.

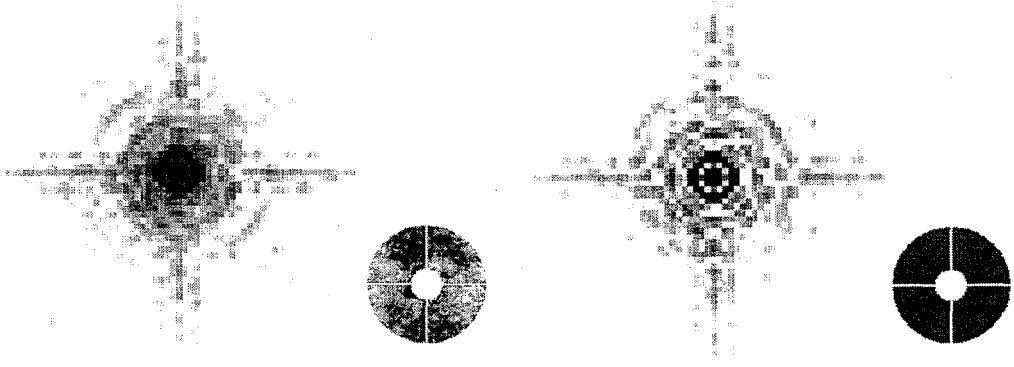

Figure 5. Internal PSF of the AO system is compared to a diffraction-limited PSF for the 3 meter telescope/IRCAL pupil. The image on the left was taken with IRCAL at 2.2 microns of a white light point source simulator (10 micron fiber) positioned at the Cassegrain focus. The wavefront image on the lower left was derived from phase diversity calculations using the PSF as input data. RMS error is 168 nm; Strehl is 0.8. One iteration of mirror flattening increases the Strehl to 0.9. The PSF image on the right is the theoretical zero aberration case.

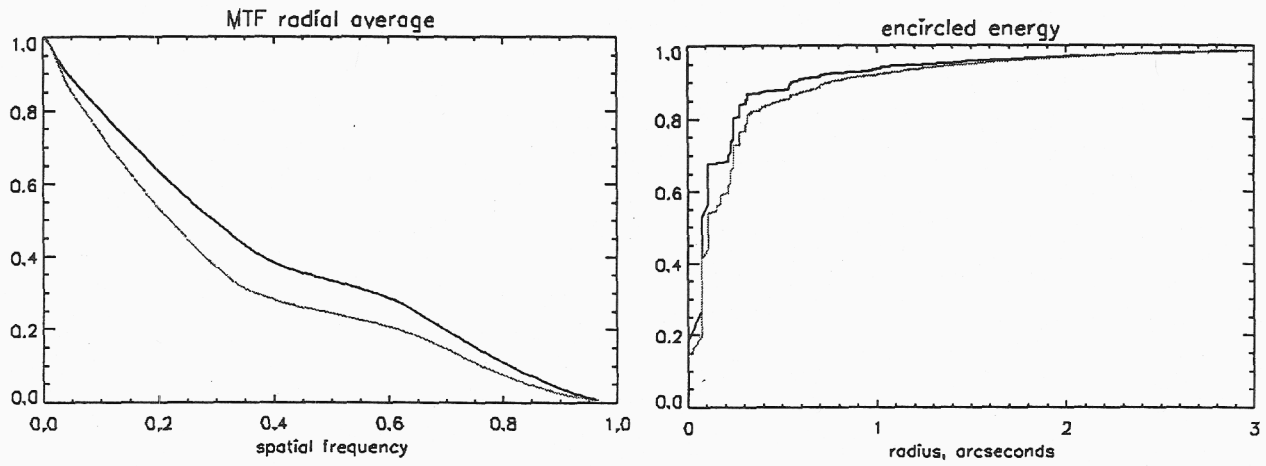

Figure 6. Modulation transfer function (MTF) and encircled energy of the internal PSF shown in Figure 5 (light line), compared to the zero aberration case (dark line).

5.2 Closed loop PSF characterization on starlight

The point-spread of starlight is reasonably symmetric and stable over time and zenith angle. There is with some degradation noticeable at zenith angles past 60 degrees, mostly low order aberration, attributable to flexure in the optical bench. Figures 7 and 8 show typical closed-loop PSFs of stars and their variation with wavelength, sky location, and brightness.

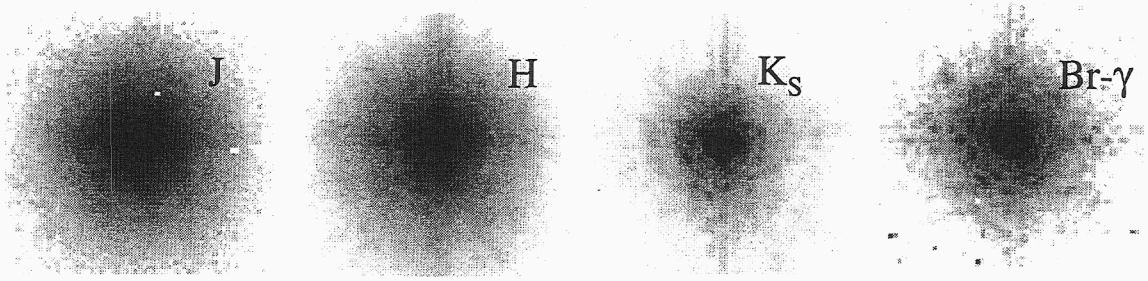

Figure 7. AO corrected PSF in various wave bands. The star is a V=9 star 35 degrees off zenith. Strehl ratios are J: 0.1, H: 0.13, K_S: 0.22, Br-γ: 0.41.

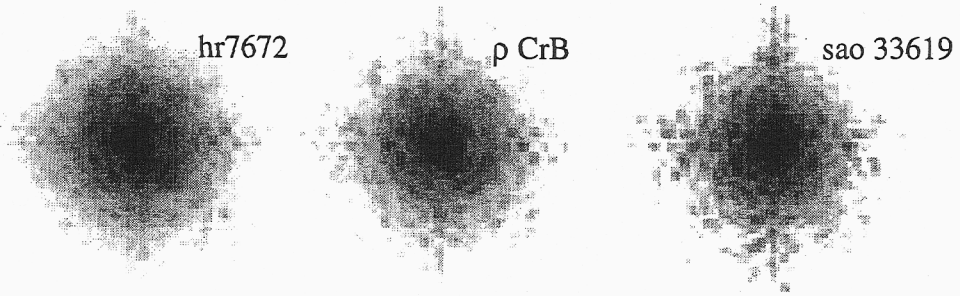

Figure 8. AO corrected PSF on different stars in the Br-γ band (2.166±.01 microns), showing stability of the PSF with time, sky location, and guide star magnitude. Hr7672 is m_V=5.8 taken on 8/2/99, ρ CrB is m_V=5.4 taken on 8/3/99, sao 33619 is m_V=9.3 taken on 8/3/99.

6. LASER GUIDE STAR ENGINEERING

In the fall of 1996, the LGS AO system demonstrated the first sodium laser guide star improved image with high-order (more than tip/tilt) adaptive optics[4]. The size of the corrected images was ~0.3 arc seconds and the Strehl ratios were ~0.1. The main error sources for these images were identified (mostly alignment of the LIRC II infrared camera) and corrected during the 1997 and 1998 runs, with the result that a LGS Strehl of greater than 0.4 was achieved in November 1998[3].

The largest error term for LGS AO is the wavefront measurement error (Table 1). This error is directly proportional to the apparent size of the guidestar on the sky. Hartmann centroiding error (related to the wavefront error through factors depending on the reconstruction algorithm and the control loop) is given by the formula[10]

$$\sigma_{\text{centroid}} = \frac{\int_{-\infty}^{\infty}\int_{-\infty}^{\infty} f(x,y)\,dx\,dy}{\sqrt{2}\int_{-\infty}^{\infty} f(0,y)\,dy} \times \frac{1}{\text{SNR}} \qquad (3)$$

where SNR is the signal-to-noise ratio of the measurement taking into account both Poisson photon noise from the star and read noise of the CCD detector. The ratio-of-integrals term has units of arcseconds on the sky; we use this as a defining measure of the spot size.

In 1998, we made a major improvement to the LGS spot size by converting the final laser amplifier to a bounce-beam design, which allowed a 25 cm diameter circular output beam instead of a 20 cm side square beam, and also tends to have better wavefront quality at high power. These both combined to reduce the spot size (as defined above) from 3 to 2 arcseconds[6].

In October 1999 our goal was to improve the launch beam quality by making sure the beam was aligned through the center of the launch telescope's optics. In the past, the beam was simply pointed so that it was boresighted it to the 3 meter, without regard to its path through the launch telescope. To eliminate any launch telescope alignment aberrations, we developed a procedure that simultaneously points the laser and keeps the launch optics aligned. However, spot size reduction beyond 2 arcseconds is difficult to measure in 1 arcsecond seeing, as shown in Figure 9. The modeling shows that the present laser guide star spot is nearly as small as the seeing conditions allow.

In the coming LGS observing campaigns, we plan to match the wavefront sensor plate scale to the 2 arcsecond LGS spot (a special set of WFS optics for LGS mode). This should allow us to use a 2×2 quad cell centroider to replace the (noisier) 4×4 arrangement we have been using until now. According to the system models this will improve signal-to-noise by 50%. When a typical set of operating conditions such as that shown in Table 1 is reoptimized by suitable choice of controller bandwidth, the overall LGS phase error will be reduced by 40 nm to 260 nm rms, corresponding to a Strehl of 0.52 at 2 microns.

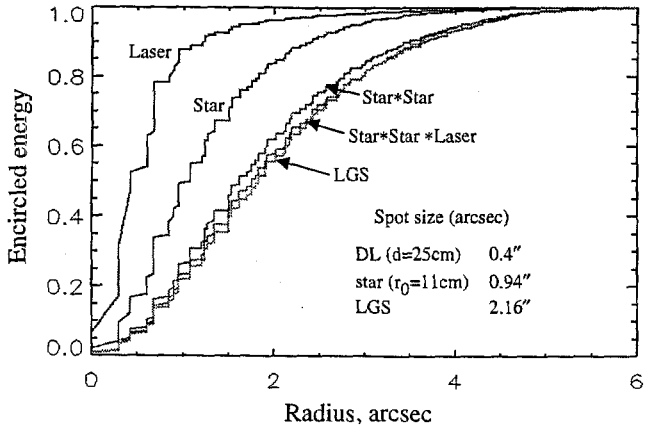

Figure 9. Laser guide star encircled energy. The "Laser" curve, derived from an internal laser wavefront diagnostic, represents the spot distribution if there were no atmosphere. The star and LGS curves were derived from field acquisition camera images. The Star*Star and Star*Star*Laser curves are models convolving the observed natural star with the no-atmosphere LGS spot (twice, once for the upgoing path, once for down path). The modeling result shows that he laser guide star is nearly as small as the seeing conditions allow.

ACKNOWLEDGMENT

This work was performed under the auspices of the U.S. Department of Energy by University of California Lawrence Livermore National Laboratory under contract No. W-740-5-Eng-48.

REFERENCES

1 Bauman, B.J., Gavel, D.T., Waltjen, K.E., Freeze, G.J., Keahi, K.A., Kuklo, T.C., Lopes, S.K., Newman, M.J., and Olivier, S.S., *New optical design of adaptive optics system at Lick Observatory*, **SPIE 3762**, 194-200, 1999.

2 Lloyd, J. P., Liu, M. C., Macintosh, B. A., Deich, W. T., Severson, S. A., Graham, J. R., *IRCAL: the infrared camera for adaptive optics at Lick Observatory*, **SPIE 4008**, March 2000.

3 Olivier, S. S., Gavel, D. T., Friedman, H.W., Max, C.E., An, J.R., Avicola, K., Bauman, B. J., Brase, J. M., Campbell, E.W., Carrano, C.J., Cooke, J. B., Freeze, G.J., Gates, E. L., Kanz, V.K., Kuklo, T.C., Macintosh, B. A., Newman, M.J., Pierce, E.L., Waltjen, K.E., and Watson, J.A., *Improved performance of the laser guide star adaptive optics system at Lick Observatory*, **SPIE 3762**, 2-7, 1999.

4 Max, C. E., Olivier, S. S., Friedman, H. W., An, J., Avicola, K., Beeman, B. V., Bissinger, H. D., Brase, J. M., Erbert, G. V., Gavel, D. T., Kanx, V. K., Liu, M. C., Macintosh, B. A., Neeb, K. P., Patience, J., Waltjen, K. E., *Image improvement from a sodium-layer laser guide star adaptive optics system*, **Science**, 277, 1649-1652, 1997.

5 Gavel, D. T., and Friedman, H. W., *Measurements of the Lick Observatory sodium laser guide star*, **SPIE 3353**, 254-259, 1998.

6 Gavel, D. T. Friedman, H. W., and Bauman, B.J., *Lick sodium laser guide star: performance during the 1998 LGS observing campaign*, **SPIE 3762**, 20-27, 1999.

7 Carrano, C. J., Olivier, S. S., Brase, J. M., Macintosh, B. A., An, J. R., *Phase retrieval techniques for adaptive optics*, **SPIE 3353**, 658-667, 1998.

8 Campbell, E. W., Bauman, B.J., Swieder, D.R., and Olivier, S.S., *High-accuracy calibration of an adaptive optics system using a phase-shifting diffraction interferometer*, **SPIE 3762**, 237-244, 1999.

9 Gavel, D. T., Bauman, B.J., Campbell, E.W., Carrano, C.J., and Olivier S.S., *Practical comparison of phase diversity to interferometry in measuring the aberrations in an adaptive optics system*, **SPIE 3762**, 266-268, 1999.

10. Tyler, G. A., and Fried, D. L., *Image-position error associated with a quadrant detector*, **J. Opt. Soc. Am.**, vol. 72, 804, 1982.